

Far-Infrared Optical Properties of CaF_2 , SrF_2 , BaF_2 , and CdF_2

D. R. BOSOMWORTH

RCA Laboratories, Princeton, New Jersey

(Received 1 December 1966)

The absorption coefficients and indices of refraction of pure CaF_2 , SrF_2 , BaF_2 , and CdF_2 at 300, 200, 80, and 5°K have been measured at all accessible frequencies between 300 Gc/sec and the transverse-optic (TO) frequencies of the crystals. The absorption has been interpreted in terms of 2-phonon difference processes involving high-energy phonons. The indices of refraction can be described by a harmonic rigid-ion approximation to the crystal. The temperature dependences of the long-wavelength dielectric constants and the TO frequencies have been measured and related to the Szigeti expression for the effective ionic charges.

I. INTRODUCTION

AS early as 1912 Rubens and Hertz¹ discovered that the room-temperature absorption at a wavelength of 300 μ in crystals of CaF_2 disappeared on cooling, the absorption coefficient being approximately proportional to the temperature. This interesting effect has not, until very recently, been studied or explained in detail. Instead, experimental and theoretical studies of the optical properties of crystals have been largely concerned with the higher-frequency regions near the fundamental lattice absorption peaks (10 to 100 μ). In these strongly absorbing regions the optical constants of CaF_2 , SrF_2 , BaF_2 , and CdF_2 (as well as other crystals) have been deduced from careful reflectivity measurements,^{2,3} and the results have been quite well described by representing the dielectric response of the lattice as a sum of classical-oscillator dispersion terms. However, the reported SrF_2 , BaF_2 , and CdF_2 results revealed subsidiary far-infrared reflection and absorption maxima ($\lambda \approx 100 \mu$) not predicted by the simple dispersion theory. Several recent theoretical discussions⁴⁻⁷ indicate that these subsidiary maxima and the strongly temperature-dependent far-infrared absorption observed by Rubens and Hertz are attributable to nonlinear and anharmonic effects which activate processes involving the simultaneous creation and destruction of two or more phonons (see Sec. III). No precise measurements over a wide range of frequency and temperature have been available to test the theory although a few far-infrared absorption

measurements on alkali halides,^{8,9} CaF_2 ,^{10,11} and SrF_2 ¹⁰ have recently been published. It is our purpose here to fill the gap by reporting direct measurements of the absorption coefficients $\alpha(\omega)$ and the indices of refraction $n(\omega)$ of CaF_2 , SrF_2 , BaF_2 , and CdF_2 at 300, 200, 80, and 5°K and all readily accessible frequencies between 3×10^{11} cps and the transverse-optic (TO) frequencies of the crystals. The temperature dependences of the "static" dielectric constants and the TO frequencies will also be reported and discussed.

II. EXPERIMENTAL METHODS AND RESULTS

All of the optical constants to be reported here were determined from transmittance measurements on approximately plane-parallel slabs of pure CaF_2 , SrF_2 , BaF_2 , and CdF_2 . Slabs cleaved or cut from commercially available single-crystal material (supplier: Harshaw Chemical Company, Cleveland, Ohio) and from boules grown in this laboratory to achieve greater sample purity gave identical results. An emission spectrographic analysis of typical samples showed that the dominant impurities in parts per million by weight were: CaF_2 -Fe (10-100), SrF_2 -Ca (500-1500), BaF_2 -Sr (200-2000), CdF_2 -Ba (≈ 5000), and Sr (≈ 5000). Some samples were polished with 1- μ alumina, others with 0.3- μ alumina. Sample thicknesses ranged from 0.3 to 10 mm.

Direct transmission measurements were made by inserting the samples in the optical path of the evacuated interferometric spectrometer¹² shown schematically in Fig. 1. The chopped output of a 100-W quartz mercury lamp *S* traversed *f*/4 input optics to arrive at the beam splitter *B* as a nearly parallel beam of radiation. The beam splitters used for these experiments were 0.001-in.- and 0.002-in.-thick Mylar films. The

† Research sponsored by the U. S. Army Durham, Durham, North Carolina, under Contract No. DA31-124-ARO-D-351, and RCA Laboratories, Princeton, New Jersey.

¹ H. Rubens and G. Hertz, *Berlin*, **14**, 256 (1912). Data reproduced by P. P. Ewald, *Naturwiss.* **10**, 1057 (1922).

² W. Kaiser, W. G. Spitzer, R. H. Kaiser, and L. E. Howarth, *Phys. Rev.* **127**, 1050 (1962).

³ J. D. Axe, J. W. Gaglianella, and J. E. Scardefield, *Phys. Rev.* **139**, A1211 (1965).

⁴ M. Lax and E. Burstein, *Phys. Rev.* **97**, 39 (1955).

⁵ H. Bilz and L. Genzel, *Z. Physik* **169**, 53 (1962).

⁶ V. V. Mitskevich, *Fiz. Tverd. Tela* **3**, 3036 (1961); **4**, 3035 (1962) [English transl.: *Soviet Phys.—Solid State* **3**, 2211 (1962); **4**, 2224 (1963)].

⁷ B. Szigeti, *Proc. Roy. Soc. (London)* **A252**, 217 (1959); *ibid.* **258**, 377 (1960).

⁸ R. Stolen and K. Dransfeld, *Phys. Rev.* **139**, A1295 (1965). This paper includes references to earlier work.

⁹ A. Hadni, J. Claudel, X. Gerbaux, G. Morlot, and J. Munier, *Appl. Opt.* **4**, 487 (1965).

¹⁰ A. Hadni, *Ann. Phys. (Paris)* **9**, 9 (1964).

¹¹ L. V. Berman and A. G. Zhukov, *Opt. i Spektroskopiya* **19**, 783 (1965) [English transl.: *Opt. Spectry* **19**, 433 (1965)].

¹² Typical expositions of the principles and methods of interferometric spectroscopy are given by Mm. J. Connes, *Rev. Opt.* **40**, 45 (1961); **40**, 116 (1961); **40**, 157 (1961); **40**, 231 (1961); P. L. Richards, *J. Opt. Soc. Am.* **54**, 1474 (1964); D. R. Bosomworth and H. P. Gush, *Can. J. Phys.* **43**, 729 (1965).

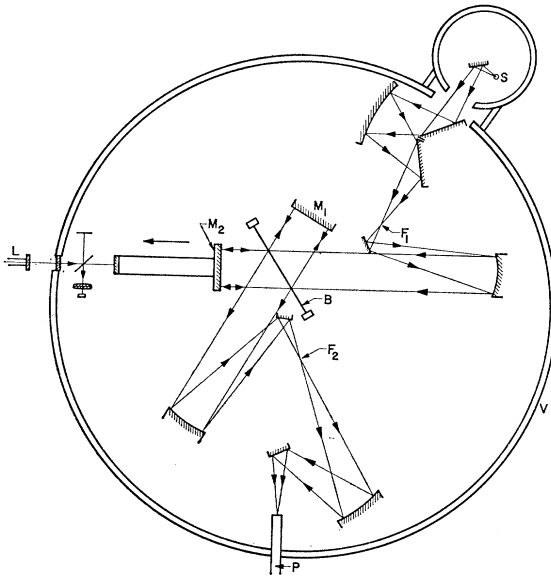


FIG. 1. A schematic cross section of the interferometric spectrometer.

resultant of the two interfering beams was focused onto the end of the light pipe P , which terminated in a liquid-helium Dewar where an electroformed copper cone condensed the beam of radiation onto a carbon bolometer at 1.7°K. The bolometer signal was amplified, synchronously demodulated, and recorded. As the plane mirror M_2 was slowly displaced normal to its surface, the system recorded a time-varying signal proportional to the autocorrelation function of the electric field of the radiation traversing the interferometer. The spectrum of the radiation was obtained by computing the cosine Fourier transform of this autocorrelation function or interferogram. A second Michelson interferometer with a 3.39- μ He-Ne laser L as a source was used to monitor the displacement of M_2 and to trigger an analog-digital system which sampled the interferogram at predetermined intervals of displacement which were multiples of 3.39 μ . The data were recorded on perforated paper tape and later transformed on the RCA-601 computer to obtain the spectra.

During room-temperature (300°K) measurements, the fluoride crystals were mounted on the warm end of the light pipe P . For measurements at lower temperatures, samples were glued with GE-7031 cement to a Dewar cold finger of solid copper in contact with liquid helium, liquid nitrogen, or a mixture of dry ice and acetone. Corresponding nominal sample temperatures of 5, 80, and 200°K will be quoted in the remainder of this paper. Although the experimentally determined absorption coefficients were independent of sample thickness, the actual temperatures of the thickest samples were probably slightly higher than the nominal values. (In a liquid-nitrogen experiment with a 1-cm-thick SrF_2 sample, the measured temperature of the

warm surface away from the cold finger was 90°K.) The Dewar was mounted on the cover of the interferometer vacuum chamber so that the samples were at the focus F_1 of the optical system.

A plane-parallel absorbing sample illuminated in vacuum by normally incident radiation of intensity I_0 transmits radiation of intensity I_T , where

$$\frac{I_T}{I_0} = \frac{(1-R)^2(1+\alpha^2\lambda^2/16\pi^2n^2)e^{-\alpha d}}{(1-Re^{-\alpha d})^2+4Re^{-\alpha d}\sin^2(2\pi nd/\lambda+\psi)}. \quad (1)$$

In this equation, $n-jk$ is the complex index of refraction, λ is the wavelength, d is the sample thickness,

$$R = \frac{(n-1)^2+k^2}{(n+1)^2+k^2} \text{ (reflectivity),} \quad (2)$$

$$\psi = \tan^{-1}2k/(n^2+k^2-1) \text{ (phase delay on reflection),} \quad (3)$$

and

$$\alpha = 4\pi k/\lambda \text{ (absorption coefficient).} \quad (4)$$

I_T and I_0 were obtained by transforming interferograms recorded with and without the fluoride samples in position. With thin and relatively transparent samples the transmission interference pattern described by Eq. (1) was readily observed; a typical pattern obtained with a 300- μ thickness of CaF_2 at 80°K is shown in Fig. 2. With strongly absorbing samples, the interference fringes tended to be obscured and distorted due to rapid variations in the mean I_T/I_0 ratio. With slightly wedged samples or thick samples studied at low resolution, Eq. (1) is effectively averaged over a range of values of λ , and the observed transmittance is

$$\frac{I_T}{I_0} = \frac{(1-R)^2(1+\alpha^2\lambda^2/16\pi^2n^2)e^{-\alpha d}}{1-R^2e^{-2\alpha d}}. \quad (5)$$

For each fluoride crystal and each temperature, thin sample transmittances described by Eq. (1) and thick sample transmittances described by Eq. (5) were measured. In every case the measured 300°K thicknesses

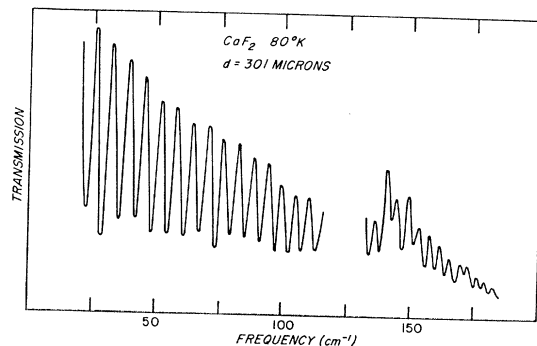


FIG. 2. Typical transmission interference fringes observed in approximately plane-parallel samples of small thickness.

were adjusted to take account of thermal contraction on cooling.

A direct solution of Eqs. (1)–(5) to obtain the desired frequency-dependent optical constants n and k (or α) is virtually impossible. In the present case this difficulty was overcome through a computational sequence which is an adaptation of methods used by Berman and Zhukov¹¹:

1. An approximate value of n was obtained by noting that transmission interference maxima and minima occur at wavelengths λ_m , such that

$$2\pi nd/\lambda_m + \psi = N\pi/2, \quad (6)$$

where N is an integer. At very long wavelengths ($\lambda > 200 \mu$) the dispersion is sufficiently small that a plot of successive values of $1/\lambda_m$ versus successive integral abscissas yields an approximately straight line of slope $1/4nd$.

2. The far-infrared transmittance of samples of thickness equal to or greater than 300μ is in practice measurable only when α is sufficiently small that $\alpha^2\lambda^2/16\pi^2n^2 \ll 1$. Therefore, Eq. (5) may for the present work be replaced by

$$\frac{I_T}{I_0} = \frac{(1-R)^2 e^{-\alpha d}}{1-R^2 e^{-2\alpha d}}. \quad (7)$$

R was approximated by $(n-1)^2/(n+1)^2$ and Eq. (7) was solved to find a preliminary value of α .

3. R was recomputed using Eqs. (2) and (4), and Eq. (7) was solved again to find improved values of α .

4. ψ was computed from Eq. (3) and found for the fluoride crystals to be $< 1^\circ$ for all wavelengths studied. Therefore, ψ could be neglected in Eq. (6), and the absolute values of N to associate with long-wavelength values of λ_m were easily determined by substituting the known value of d and the approximate value of n .

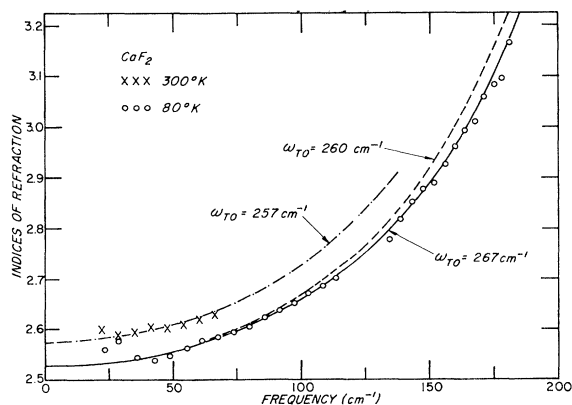


FIG. 3. The points show experimental values. The lines show theoretical curves fitted to the experimental data by adjusting ϵ_0 and ω_{T0} in Eq. (8).

$$n(\omega) = ((\epsilon_0\omega_{T0}^2 - \epsilon_\infty\omega^2)/(\omega_{T0}^2 - \omega^2))^{1/2}.$$

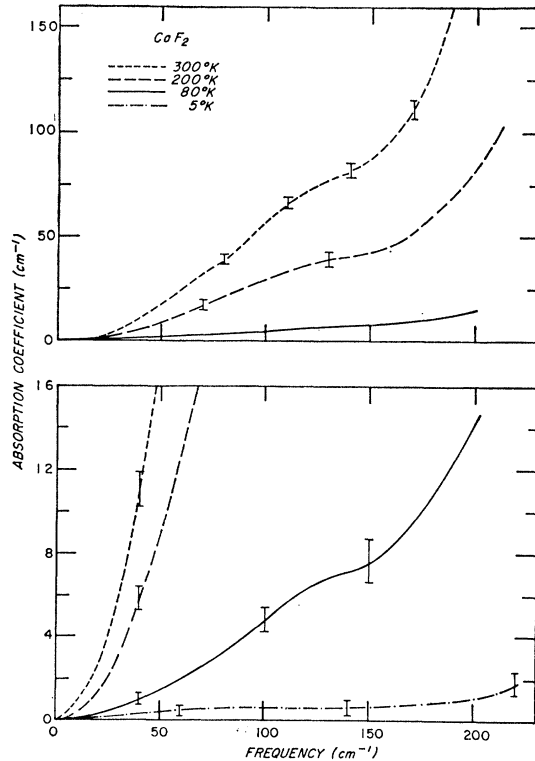


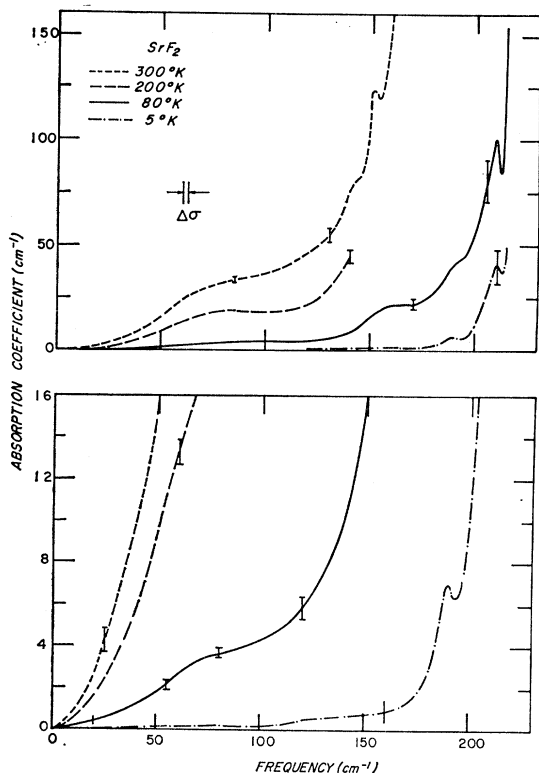
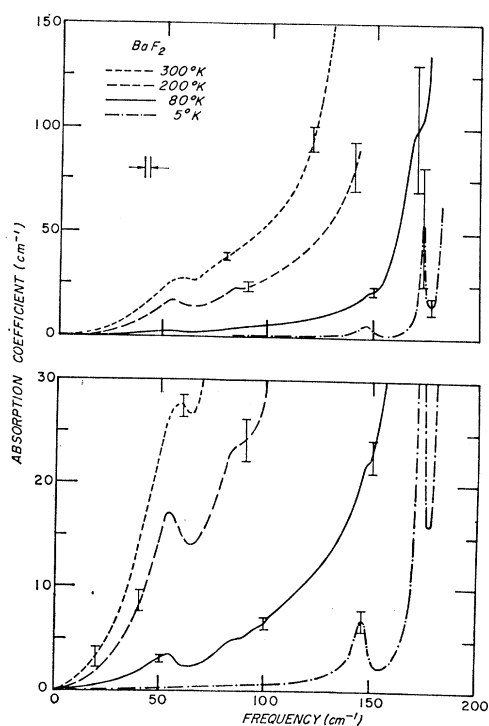
FIG. 4. The absorption coefficient of CaF_2 crystals at four temperatures. The vertical bars indicate probable errors. The limit of resolution was $\Delta\sigma = 2.5 \text{ cm}^{-1}$. Frequency-dependent indices of refraction were used to take proper account of reflection losses.

Shorter-wavelength extrema were associated with successively larger integers.

5. Knowing N and d , Eq. (6) was solved to obtain precise values of n at each wavelength λ_m . The frequency-dependent index for refraction determined in this manner for CaF_2 at 80°K is shown by the points in Fig. 3. Similar data were obtained for SrF_2 , BaF_2 , and CdF_2 . The lines in Fig. 3 are theoretical curves which will be discussed later.

6. Finally, R was computed using the frequency-dependent indices of refraction, and Eq. (7) was solved to find the final values of α . The results for CaF_2 , SrF_2 , BaF_2 , and CdF_2 are shown in Figs. 4–7, respectively.

The probable error in the measured absorption coefficients as determined from the average deviation of several experiments is indicated by the vertical bars in Figs. 4–7. In most spectral regions samples of three or more different thicknesses were examined. The absence of any systematic variations of the absorption coefficients with sample thickness indicated that the results were not influenced by surface scattering or thickness-dependent sample temperatures. Sample thicknesses which yielded transmittances between 4 and 40% were used whenever possible because there must be appreciable attenuation to obtain accurate absorption coeffi-

FIG. 5. The absorption coefficients of SrF₂.FIG. 6. The absorption coefficients of BaF₂.

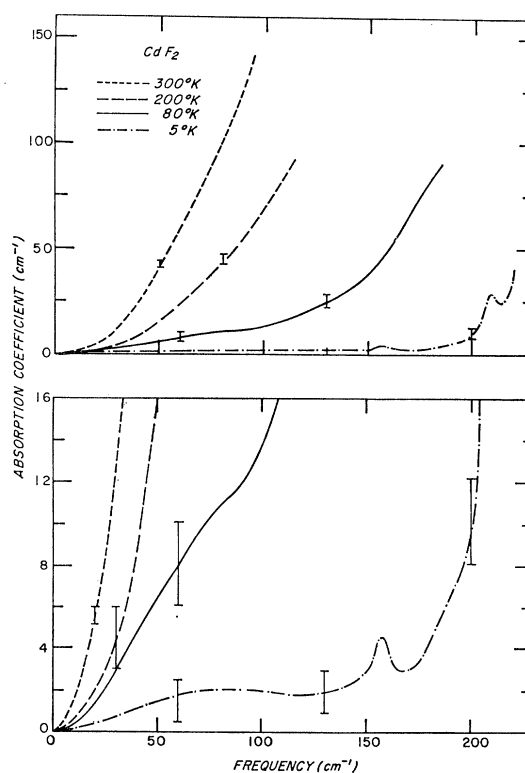
coefficients. At 5°K the observed attenuation, even with the thickest available samples, was small in most spectral regions; the 5°K curves at low frequencies serve primarily to indicate an upper limit on the absorption coefficient. At all temperatures a large part of the uncertainty in the absolute value of the absorption coefficient arises because the detector sensitivity and the amplifier gain are never perfectly stable with the result that I_0 and I_T are not recorded under identical conditions. This effect does not appreciably influence the frequency dependence of the absorption spectra; the structural features shown in Figs. 4-7 are more reliable than the error bars might seem to indicate. In most of these experiments the limit of resolution, $\Delta\sigma$, was 2.5 cm^{-1} ; the sharp high-frequency structure in SrF₂, BaF₂, and CdF₂, was studied with $\Delta\sigma=1 \text{ cm}^{-1}$.

III. THEORETICAL BACKGROUND

The exact expression for the infrared dielectric constant of an infinite harmonic fluorite lattice is¹³

$$\epsilon(\omega) = (\epsilon_0\omega_{TO}^2 - \epsilon_\infty\omega^2) / (\omega_{TO}^2 - \omega^2), \quad (8)$$

where $\epsilon(\omega)$ is the dielectric constant at the frequency ω , ϵ_∞ is the electronic contribution to the dielectric constant at infrared frequencies, ϵ_0 is the electronic and

FIG. 7. The absorption coefficients of CdF₂.

¹³ M. Born and K. Huang, *Dynamical Theory of Crystal Lattices* (Clarendon Press, Oxford, England, 1954), Chap. 2.

ionic contribution to the dielectric constant at microwave frequencies, and ω_{TO} is the infrared-active TO vibrational frequency at zero wave vector ($\mathbf{k}=0$). In the frequency region of the present experiments, ($\omega < \omega_{\text{TO}}$), Eq. (8) predicts dispersion without attenuation; it does not describe the measured absorption coefficients shown in Figs. (4)–(7).

All real crystals are anharmonic in the sense that the potential energy corresponding to an arbitrary distortion of the lattice depends on cubic and higher powers of the normal coordinates.¹⁴ Moreover, the ions in a real crystal are deformed in the course of lattice vibrations and this causes nonlinear terms in the crystal dipole moment. These effects have been considered by several authors^{4–7,14–17} who have shown that anharmonicity and nonlinearity give rise to multi-phonon processes which are not restricted to $\mathbf{k}=0$ in the Brillouin zone. In this work, only 2-phonon processes need be considered because of the high Debye temperatures of the crystals studied.^{8,17} In the 2-phonon difference process, a phonon of frequency ω_l is destroyed and a phonon of frequency ω_k is created, the difference in energy being supplied by an absorbed photon of frequency $\omega = \omega_k - \omega_l$ and momentum being conserved provided that $\mathbf{k}_k = \mathbf{k}_l$. In the 2-phonon sum process an absorbed photon of frequency ω creates phonons of frequencies ω_i and ω_j , where $\mathbf{k}_i = -\mathbf{k}_j$. At high temperatures both processes yield contributions proportional to the temperature T . When $T \rightarrow 0$, the sum process remains active but no phonons exist in the crystal and absorption via the 2-phonon difference disappears.

IV. DISCUSSION OF RESULTS

A. Absorption Coefficients

At frequencies less than ω_{TO} the absorption coefficients of CaF_2 , SrF_2 , BaF_2 , and CdF_2 are strongly temperature dependent (Figs. 4–7). At frequencies up to approximately 80% of ω_{TO} , the measurements on all four materials yield α -versus- T curves of the form shown by the heavy solid lines in Fig. 8. At very low temperatures the absorption is essentially zero; it rises rapidly between 50 and 200°K and then levels off to become nearly linear in T at temperatures of the order of 300°K. The high-temperature behavior is typical of 2-phonon absorption processes. The low-temperature behavior indicates that the 2-phonon difference process is the dominant absorption mechanism.

At a particular frequency ω , the dependence of α on T in the 2-phonon difference process is almost entirely determined by an occupation number factor ($\bar{n}_l - \bar{n}_k$),

where

$$\bar{n}_i = [\exp(\hbar\omega_i/kT) - 1]^{-1}. \quad (9)$$

Because $\omega_k = \omega + \omega_l$, this factor is a function of the two variables ω_k and T . For any chosen value of ω_k , a curve of α versus T may be computed and compared with the experimental results. It was found that ($\bar{n}_l - \bar{n}_k$) evaluated for properly chosen values of ω_k reasonably reproduced the form of the experimental temperature dependence at temperatures greater than 100°K. This is demonstrated by the dashed curves in Fig. 8. The agreement between the experimental and theoretical curves supports the 2-phonon difference process interpretation and at the same time serves to determine approximately the mean frequency of the phonons involved in the initial and final states. In CaF_2 , for example, a value of ω_k of the order of 350 cm^{-1} best describes the high-temperature absorption. Referring to the CaF_2 dispersion diagrams,¹⁸ we conclude that low-wave-vector acoustic phonons do not contribute significantly to this absorption. Studies of alkali halide crystals have led to a similar conclusion.⁸ The appropriate value of ω_k appears to be relatively independent of ω at frequencies below $0.8\omega_{\text{TO}}$. Because the frequencies of optical modes tend to be independent of wave vector while the frequencies of acoustic modes are not, this suggests that the dominant absorption process involves the annihilation of acoustic phonons and the creation of optic phonons. The magnitude of ω_k suggests that the creation of phonons belonging to Raman-active branches may play an important role. In SrF_2 and BaF_2 the appropriate values of ω_k are smaller, as one would expect on the basis of the smaller observed TO and LO frequencies.

Below 100°K the dashed curves in Fig. 8 fall below the experimental data. The difference may reasonably be explained as a contribution due to transitions involving phonons of much lower energy. These would presumably be acoustic phonons in which case the only allowed transitions are those in which transverse acoustic (TA) phonons are destroyed and higher-energy longitudinal acoustic (LA) phonons are created.¹⁴

At low frequencies the measured absorption coefficients are proportional to ω^2 . At higher frequencies all of the spectra show definite structural features. These features can be divided into two distinct classes; those well removed from ω_{TO} are broad and they vanish as $T \rightarrow 0^\circ\text{K}$; those close to ω_{TO} are sharper and they persist even at 5°K. The low-frequency structure is due to the frequency dependence of the 2-phonon difference process with absorption maxima corresponding to peaks in the 2-phonon density of states. Although this density of states is not known, it is obvious that peaks will usually occur when two branches of the phonon-dispersion curves are parallel, as they are, for example, at the zone boundary. The high-frequency structure,

¹⁴ D. H. Martin, *Advan. Phys.* **14**, 39 (1965). This article gives an excellent review of the spectroscopy of crystal lattices including the effects of anharmonicity and nonlinearity.

¹⁵ M. Lax, *J. Phys. Chem. Solids* **25**, 487 (1964).

¹⁶ R. A. Cowley, *Advan. Phys.* **12**, 421 (1963).

¹⁷ W. Zernik, *Rev. Mod. Phys.* **39**, 432 (1967).

¹⁸ S. Ganesan and R. Srinivasan, *Can. J. Phys.* **40**, 74 (1962).

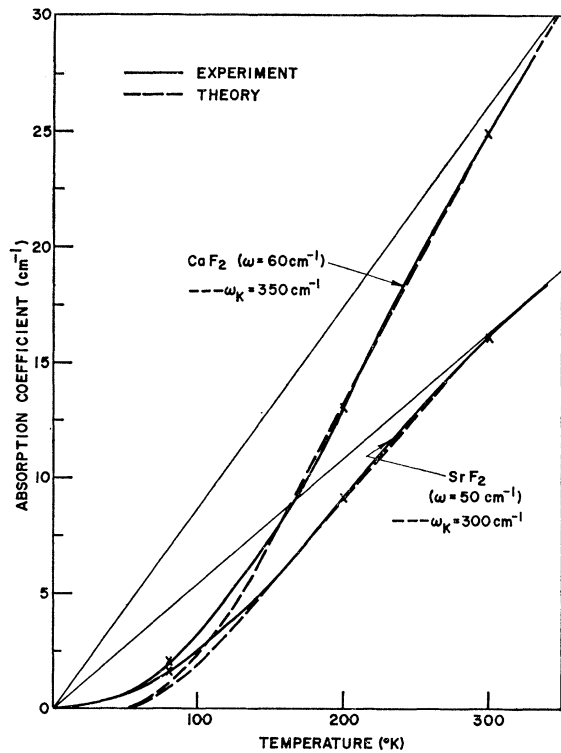


FIG. 8. Typical temperature variations of the absorption coefficients. The dashed theoretical curve is the occupation number factor $(\bar{n}_l - \bar{n}_k)$ normalized to agree with the experimental point at 300°K. The straight lines indicate the linear high-temperature asymptotes of the experimental curves.

which is not so well understood, is probably due to 2-phonon sum processes associated with anharmonic terms in the potential energy.^{14,16}

Although comparable features appear in the spectra of the four materials studied, there is no obvious corre-

lation between the frequencies of the absorption peaks observed in different crystals.

The far-infrared absorption coefficient of CdF₂ is larger than that of the alkaline earth fluorides. This is compatible with the strongly damped dielectric response determined from CdF₂ reflectivity measurements.³ There are only small differences in the magnitudes of the absorption coefficients of CaF₂, SrF₂, and BaF₂, with SrF₂ being slightly more transparent than the other two. The structure in the spectra is sharper when the mass of the alkaline-earth ion is large.

B. Indices of Refraction and TO Frequencies

Because absorption in the reststrahlen region far exceeds that at longer wavelengths it is reasonable to expect that Eq. (8) will describe the far-infrared index of refraction $n(\omega) = \epsilon(\omega)^{1/2}$ of CaF₂, SrF₂, BaF₂, and CdF₂. This was found to be the case as shown by the curves in Fig. 3. The validity of Eq. (8) has subsequently been checked by Zernik,¹⁷ who fitted a phenomenological frequency-dependent damping function^{15,3} to the absorption-coefficient data in Figs. 4-7; this damping function was then incorporated into the corresponding expressions for the index of refraction and shown to produce negligible deviations from the result based on the harmonic approximation.

In fitting Eq. (8) to the experimental data there are essentially two unknowns, ϵ_0 and ω_{TO} , which can be determined on the basis of two measured quantities, the magnitude of the refractive index and its dispersion. At 80°K this was easily accomplished with the results shown in Table I.^{2,3,12,19-21} Because the dispersion depends strongly on ω_{TO} as illustrated by the curves computed using $\omega_{TO} = 260$ and 267 cm^{-1} (Fig. 3), this is an accurate and convenient way of determining the low-temperature transverse optic frequencies. Measure-

TABLE I. Infrared optical constants of CaF₂, SrF₂, BaF₂, and CdF₂. The values of n_0 and ϵ_0 at all temperatures and ω_{TO} at 80°K are experimental results. Values of ω_{TO} at 300°K were taken from Ref. 2 for CaF₂, SrF₂, and BaF₂ and from Ref. 3 for CdF₂. The value of ϵ_∞ for CaF₂ was taken from Ref. 12, and for BaF₂ from Ref. 20 with the temperature dependences from Ref. 21. For SrF₂ the value of ϵ_∞ quoted in Ref. 2 was used and for CdF₂ the value recommended in Ref. 3. ω_{LO} was calculated using the Lyddane-Sachs-Teller relation (Ref. 19).

	Temp. °K	ϵ_∞	n_0	ϵ_0	$\omega_{TO} (\text{cm}^{-1})$	$\omega_{LO} (\text{cm}^{-1})$
CaF ₂	300	2.040±0.001	2.575±0.015	6.63±0.08	257	463
	200	2.044	2.555±0.015	6.53±0.08		468
	80	2.047	2.525±0.015	6.38±0.08	267±2	472
SrF ₂	300	2.07	2.490±0.015	6.20±0.07	217	381
	80	2.07	2.457±0.017	6.04±0.08	225±2	384
BaF ₂	300	2.150±0.001	2.635±0.015	6.94±0.08	184	331
	80	2.157	2.561±0.017	6.56±0.09	189±2	330
CdF ₂	300	2.40	2.914±0.015	8.49±0.09	202	380
	80	2.40	2.790±0.017	7.78±0.10	224±3	403

¹⁹ R. Lyddane, R. Sachs, E. Teller, Phys. Rev. **59**, 673 (1941). ω_{LO} is the frequency of LO phonons at $\mathbf{k}=0$.

²⁰ I. H. Malitson, J. Opt. Soc. Am. **54**, 628 (1964).

²¹ T. W. Houston, L. F. Johnson, P. Kisliuk, and D. J. Walsh, J. Opt. Soc. Am. **53**, 1286 (1963).

ments at 80 and 5°K yielded values which were identical to within the experimental error. At high temperatures the dispersion could only be measured over a limited range of frequencies and ω_{TO} could not be determined from the experimental data. In this case the published 300°K values of ω_{TO} were assumed to be correct and curves computed using these were fitted to the experimental points to obtain ϵ_0 .

The methods used here yield a direct determination of dielectric constants ϵ_0 , which are characteristic of the vibrations of the lattice and its constituent ions. As such they are of considerable interest because values of ϵ_0 determined by conventional low-frequency capacitance methods can be significantly inflated by low-frequency contributions due to the migration of lattice defects. For CaF_2 , SrF_2 , and BaF_2 the direct values in Table I are considerably smaller than those obtained from capacitance measurements made several years ago²² (when good crystals were not readily available) and slightly smaller than those reported more recently.² It should be noted, however, that the values of ϵ_0 determined from a Kramers-Kronig dispersion analysis of reflectivity data are in reasonable agreement with the present results.²

The measured 80°K TO frequencies are appreciably larger than the values reported at 300°K, especially in the case of CdF_2 . Qualitatively, such shifts in the lattice frequencies are quite reasonable; as the lattice contracts, the distances between ions decrease and the forces between ions increase. Quantitatively, the TO lattice frequencies of crystals can be related to the corresponding elastic and dielectric constants, as first shown by Szigeti.^{23,24} The experimental results can be used to check the validity of these relations and the underlying assumptions and models on which they are based.

For example, consider the Szigeti expression for the effective charge²³ in the form appropriate to a harmonic fluorite lattice:

$$e^* = se = \frac{3c\omega_{\text{TO}}[\pi V\mu(\epsilon_0 - \epsilon_\infty)]^{1/2}}{2(\epsilon_\infty + 2)}. \quad (10)$$

In Eq. (10), V is the volume of a primitive cell, e is the electronic charge, c is the velocity of light, and μ is the reduced mass of the positive and negative ions in the primitive cell, $\mu = 2M^+M^-(M^+ + 2M^-)$. The dimensionless factor s commonly differs from unity because short-range mechanical forces distort the nonrigid ions as they are displaced relative to one another, and the lattice polarization is correspondingly different than it would be if each ion moved as a rigid unit. In fact, Axe

TABLE II. Quantities pertinent to the Szigeti relationship [Eq. (11)] connecting ω_{TO} and ϵ_0 with the effective charge e^* . The effective charge on the metal ion is $2e^*$.

	Temp. °K	$\omega_{\text{TO}}^2 V(\epsilon_0 - \epsilon_\infty)$ (10^{-20} cm)	$S = e^*/e$
CaF_2	300	1236	0.823
	80	1246±30	0.824
SrF_2	300	979	0.847
	80	1001±30	0.857
BaF_2	300	959	0.870
	80	920±27	0.852
CdF_2	300	978	0.812
	80	1053±34	0.841

has shown²⁵ that a dipole shell model of the ions²⁶ yields exactly the relation in Eq. (10). Because the effective charge is not likely to be temperature-dependent, Eq. (10) predicts to a good approximation that

$$\omega_{\text{TO}}^2 \propto 1/V(\epsilon_0 - \epsilon_\infty). \quad (11)$$

This relation, which is reasonably confirmed by the available data as shown in Table II, provides a convenient correlation of values of ω_{TO} and ϵ_0 . The agreement is not very good in the case of CdF_2 and this may indicate the influence of anharmonic effects. However, no definite statements are possible because the probable error in ω_{TO} at 300°K is not known and the value of ϵ_0 is somewhat uncertain.

The values of the effective charge are themselves quite interesting. In CaF_2 , SrF_2 , and BaF_2 the present results reasonably confirm the values given by Axe.²⁵ However, in the case of CdF_2 , the present value of ϵ_0 is larger than the value used by Axe *et al.*,³ and we find a correspondingly larger effective charge. The earlier value of e^* indicated that the alkaline-earth fluorides satisfied a qualitative linear relation between the effective charge and the electronic polarizability of the ions²⁷ while CdF_2 did not. The difference was attributed to reduction of the static charge due to covalent bonding effects. The present value of e^* suggests that the covalent bonding effects are smaller than previously indicated.

ACKNOWLEDGMENTS

These measurements were made with the conscientious technical assistance of R. B. Marotte. The encouragement of Dr. Z. J. Kiss and many helpful discussions with Dr. W. Zernik were greatly appreciated.

²² K. Hojendahl, Klg. Danske Videnskab. Selskab, Mat.-Fys. Medd. **16**, 2 (1938).

²³ B. Szigeti, Trans. Faraday Soc. **45**, 155 (1949).

²⁴ B. Szigeti, Proc. Roy. Soc. (London) **A204**, 51 (1950).

²⁵ J. D. Axe, Phys. Rev. **139**, A1215 (1965).

²⁶ B. G. Dick and A. W. Overhauser, Phys. Rev. **112**, 90 (1958).

²⁷ J. D. Axe and G. D. Pettit, J. Phys. Chem. Solids **27**, 621 (1966).